Published in final edited form as:
Mol Pharm. 2009 ; 6(3): 959–970. doi:10.1021/mp8002682.

Biorecognition and Subcellular Trafficking of HPMA Copolymer - Anti-PMSA Antibody Conjugates by Prostate Cancer Cells

Jihua Liu[1], **Pavla Kopečková**[1,2], **Patrick Bühler**[3], **Philipp Wolf**[3], **Huaizhong Pan**[1], **Hillevi Bauer**[1], **Ursula Elsässer-Beile**[3], and **Jindřich Kopeček**[1,2]

1*Department of Pharmaceutics and Pharmaceutical Chemistry, University of Utah, Salt Lake City, UT, USA*

2*Department of Bioengineering, University of Utah, Salt Lake City, UT, USA*

3*Department of Urology, Experimental Urology, University of Freiburg, Freiburg, Germany*

Abstract

A new generation of antibodies against the prostate specific membrane antigen (PSMA) has been proven to bind specifically to PSMA molecules on the surface of living prostate cancer cells. To explore the potential of anti-PSMA antibodies as targeting moieties for macromolecular therapeutics for prostate cancer, fluorescently labeled HPMA (*N*-(2-hydroxypropyl)methacrylamide) copolymer - anti- PSMA antibody conjugates (P-anti-PSMA) were synthesized and the mechanisms of their endocytosis and subcellular trafficking in *C4-2* prostate cancer cells were studied. Radioimmunoassays showed the dissociation constants of P-anti-PSMA for *C4-2* prostate cancer cells in the low nanomolar range, close to values for free anti-PSMA. It indicated that conjugation of anti-PSMA to HPMA copolymers did not compromise their binding affinity. The rate of endocytosis of P-anti-PSMA was much faster than that of control HPMA copolymer conjugates containing non-specific IgG. Selective pathway inhibitors of clathrin-mediated endocytosis and of macropinocytosis inhibited the internalization of P-anti-PMSA. Inhibition of clathrin-mediated endocytosis was further evidenced by down-regulation of clathrin heavy chain expression by siRNA. Using a dominant-negative mutant of dynamin (Dyn K44A) to abolish the clathrin-, caveolae-independent endocytic pathway, we found that some of P-anti-PSMA adopted this pathway to be endocytosed into C4-2 cells. Thus multiple receptor-mediated endocytic pathways, including clathrin-mediated endocytosis, macropinocytosis, and dynamin-independent endocytosis, were involved in the internalization of P-anti-PSMA. The extent of the participation of each pathway in P-anti-PSMA endocytosis was estimated. Membrane vesicles containing P-anti-PSMA rapidly co-localized with membrane vesicles overexpressing Rab7, a late endosome localized protein, demonstrating that a part of P-anti-PSMA was transported to late endosomes.

Keywords

HPMA copolymer; drug delivery; antibody targeting; endocytosis; clathrin-mediated endocytosis

Introduction

Polymer therapeutics including polymer-protein conjugates, drug-polymer conjugates, supramolecular, and other nanosized drug delivery systems represent a compensatory and

Correspondence to: Jindřich Kopeček.

CORRESPONDING AUTHOR FOOTNOTE: Department of Pharmaceutics and Pharmaceutical Chemistry University of Utah 30 S. 2000 E. Rm. 201 Salt Lake City, Utah 84112-5820 U.S.A. Phone: (801) 581-7211 Fax: (801) 581-7848 E-mail: E-mail: Jindrich.Kopecek@utah.edu.

promising approach on the improvement of cancer treatment, due to lack of tumor selectivity of most low-molecular-weight anticancer chemotherapeutic agents. Conjugating low-molecular-weight anticancer drugs to polymers establishes (passive) tumor selectivity due to the enhanced permeability and retention (EPR) effect.[1] However, one way to achieve high local concentration of polymer therapeutics in tumor tissues is incorporation of a targeting moiety able to actively guide polymer therapeutics to the tumor sites.[2] Clinical success of monoclonal antibodies bodes well for their use as targeting moieties[3] in drug delivery systems. Indeed, targeted polymer therapeutics have improved the therapeutic index with minimal side effects in both preclinical and clinical settings.[4-7]

The incorporation of OV-TL16 antibody, recognizing the CD47 (OA-3) antigen expressed on most of human ovarian carcinomas, into *N*-(2-hydroxypropyl)methacrylamide (HPMA) copolymer based polymer therapeutics resulted in their enhanced accumulation in human ovarian OVCAR-3 carcinoma xenografts with concomitant decrease in tumor proliferation.[2] More efficient tumor targeting and higher antitumor efficacy were demonstrated in targetable HPMA copolymer-drug conjugates mediated by Fab' antibody fragment from OV-TL16 antibody than the non-targeted HPMA copolymer drug conjugate.[8]

Identification of tumor cell surface specific molecules enables to develop targeted anticancer polymer therapeutics. Prostate-specific membrane antigen (PSMA) is highly expressed in prostate cells with a minimal expression in tissues of the brain, proximal small intestine, salivary glands, and kidney.[9-11] The expression of PSMA is upregulated in malignant disease, with the greatest level detected in metastatic androgen independent prostate cancer.[12,13] It has been found also abundantly expressed in tumor-associated neovasculature in a variety of solid tumors.[10,14] PSMA is a dimeric Type II integral membrane glycoprotein with an intracellular segment, a transmembrane domain, and an extracellular domain.[11]

Recently, Elsässer-Beile and coworkers developed a new generation of monoclonal and recombinant antibodies against cell-adherent PSMA.[15] In their studies, mAbs and scFv from mice immunized with the native form of PSMA demonstrated binding activity and internalization into LNCaP cells.[15] In addition, the antibodies possessed great specificities, verified by lack of binding activity toward a variety of PSMA-negative cells. A recombinant immunotoxin based on the anti-PSMA antibody possessed selective toxicity to prostate cancer cells.[16,17] Moreover, a bispecific diabody against PMSA and CD3 was active in T-cell mediated lysis of prostate cancer cells.[18]

In addition of antibodies, aptamers, synthetic oligonucleotides, were identified as capable of binding to PSMA.[19] Highly selective and effective therapeutic modalities based on aptamers have been developed to deliver chemotherapeutics, functional siRNA and toxin for the treatment of prostate cancer.[20-25] Aptamer-based macromolecules as cellular imaging and cellular labeling agents also have been investigated.[26,27]

PSMA, presumably like other cell surface receptors, undergoes internalization constitutively upon binding to its putative ligand. This process is referred to as receptor-mediated endocytosis, in which more and more elaborate mechanisms have been recognized and characterized recently.[28] Nevertheless, how the PSMA directs the conjugates to be endocytosed into the tumor cells once it is bound to polymer carriers as a targeting moiety has not been investigated.

Pinocytosis, the fluid-phase endocytosis, has been recently recognized to occur in all cells by at least four basic mechanisms: clathrin-mediated endocytosis (CME),[29] caveolae-mediated endocytosis,[30] clathrin- and caveolae-independent endocytosis,[28,31] and macropinocytosis.[32] These pathways differ with regard to the nature of the cargo, the mechanism of vesicle formation, the regulation of cargo entry, and especially, the ultimate intracellular destinations of cargo.[28,33]

CME occurs constitutively in all mammalian cells[31] and continuously takes up essential nutrients, such as transferrin and low-density lipoprotein. Cargoes internalized by cells through CME are subsequently transported to early endosomes, from which some cargo is recycled back to the plasma membrane, whereas other consignments are delivered to late endosomes, and ultimately, lysosomes for degradation.[29] The caveolae-mediated endocytic pathway is less defined than CME. Caveolae is a non-coated flask shaped membrane invagination, which is formed by an assembly of glycosphingolipids and cholesterol (lipid raft) and the integrated transmembrane protein caveolin. Two well-studied ligands of this pathway are cholera toxin subunit B (CTX) and SV40 simian virus; CTX eventually targets to Golgi and SV40 to the endoplasmic reticulum.[30,34] Macropinocytosis is traditionally considered to involve the internalization of large size macromolecules or significant amounts of fluid together with large areas of plasma membrane. However, it is actin-dependent and regulated by phosphoinositide (PI) 3-kinases.[35] The mechanisms that govern caveolae- and clathrin-independent endocytosis remain largely unknown. One of distinction that can be used to define this pathway is the independency of dynamin, a GTPase protein surrounding the neck of vesicle pits to mediate the scission of a wide range of vesicles such clathrin-coated vesicles and caveolae.[31,36]

The importance of understanding endocytic pathways involved in the internalizaton and subcellular trafficking of polymer-drug conjugates has been greatly appreciated recently. [37, 38] For example, one can design efficient endosomal escape or lysosomal enzymatic cleavage based on the trafficking and localization of polymer-drug conjugates. One also can optimize the physico-chemical characteristics of polymer-drug conjugates to guide them to the proper membrane limited subcellular organelle. In the present study, the endocytic mechanisms and subcellular trafficking of HPMA copolymer - anti-PSMA antibody conjugates were investigated in depth in live cells.

Experimental Section

Materials

Alexa Fluor 633 labeled transferrin, Alexa Fluor 647-labeled dextran 10 kDa and Hoechst 33342 were purchased from Molecular Probes (Carlsbad, CA). Chlorpromazine, filipin complex, meviolin, 5-(*N*-ethyl-*N*-isopropyl)-amiloride, LY 294002, and wortmannin were from Sigma- Aldrich (St. Louis, MO). Clathrin HC siRNA and control siRNAs were purchased from Santa Cruz Biotechnology (Santa Cruz, CA). Lipofectamine 2000 was from Invitrogen (Carlsbad, CA). The plasmid encoding EGFP-dynamin wild type (EGFP-dynamin^{WT}) and dynamins deficient mutant plasmid (EGFP-dynamin^{K44A}) were gifts from Dr. Diane McVey Ward (University of Utah). The plasmids encoding EYFP-Rab5 and EYFP-Rab7 were kindly provided by Dr. Xiaowei Zhuang (Harvard University). LNCap derived androgen independent C4-2 cells and the prostate cancer cell line PC-3 were purchased from American Type Culture Collection (ATCC) (Manassas, VA). Fetal bovine serum was from Hyclone (Logan, UT). C4-2 and PC-3 cells were maintained in RPMI 1640 medium supplemented with 10% fetal bovine serum at 37°C in an incubator with 5% CO_2. The sterile 35 mm petri dish with 14mm glass bottom microwell for confocal microscopy was from MatTek Corporation (Ashland, MA). Three monoclonal antibodies against different epitopes of PSMA (3A/12, 3F/11, 3E/7) were generated as previously described.[15] In the present study, all the data were generated with PSMA (3A/12) and its polymeric counterpart (P-anti-PSMA) except the determination of the antigen binding affinity.

Methods

UV-Vis spectra were measured on a Varian Cary 400 Bio UV-Visible Spectrophotometer. Mass spectra of all synthesized compounds were obtained using a mass spectrometer Voyager-DE (STR Biospectrometry Workstation, PerSeptive Biosystems, Framingham, MA). The

molecular weight and molecular weight distribution of polymers were measured on the ÄKTA FPLC system (GE Healthcare, formerly Amersham) equipped with UV and RI detectors using a Superose 6 HR10/30 column with PBS (pH 7.4) as the mobile phase. The average molecular weights were calculated using a calibration with polyHPMA fractions.

Synthesis of HPMA copolymer - antibody conjugates

The conjugates were prepared in several steps (Fig. 1). Polymeric precursors containing reactive thiazolidine-2-thione (TT) groups for binding antibody were synthesized by solution radical copolymerization of monomers in DMSO. The comonomers, HPMA (key monomer unit), MA-Gly-Gly-TT (*N*-methacryloylglycylglycine thiazolidine-2-thione; monomer unit bearing reactive TT group at the end of diglycine spacer[39]) and MA-FITC ((5-[3-(methacryloylaminopropyl)thioureidyl]fluorescein; monomer unit containing FITC[40]), were prepared as previously described. In the last step, the antibodies were coupled to the polymer precursors by aminolysis of TT groups in PBS.

Synthesis of reactive polymer precursors

Polymer precursor containing TT and FITC (P-FITC-TT) was prepared by polymerization of HPMA (270 mg, 94.5 mol%), MA-GG-TT (31 mg, 5 mol%), MA-FITC (5.3 mg, 0.5 mol %) and 20 mg AIBN in 1.8 mL DMSO containing 10 μl CH_3COOH. After purification by re-precipitation into acetone the polymer contained 0.32 mmol TT/g (4.9 mol % TT; determined by UV spectrophotometry using extinction coefficient of monomer 10800 $M^{-1}cm^{-1}$ in MeOH, 305 nm) and 0.027 mmol FITC/g (0.4 mol %); yield 0.25 g; Mw 42 kDa, M_w/M_n 1.5. Polymer precursor containing Texas Red (P-TxR-TT) was prepared from precursor containing only TT groups (prepared exactly as the P-FITC-TT omitting the MA-FITC in the polymerization mixture) by modifying a small amount of reactive TT groups by Texas Red cadaverin (Molecular Probe Texas Red®C_5). Briefly, 100 mg of polymer precursor containing 0.038 mmol TT groups was dissolved in 0.5 mL DMSO, 1.7 mg (0.0025 mmol) of Texas Red cadaverin was added and stirred for 30 min at room temperature (r.t.). The polymer was precipitated into acetone and dried. The content of TxR groups was 0.022 mmol/g (0.35 mol %; extinction coefficient 86000 $M^{-1}cm^{-1}$ in PBS, 593 nm).

Binding of anti-PSMA Ab to polymer precursors

Typical procedure was as follows: The polymer precursor (2 mg) was dissolved in 50 μl deionized H_2O and mixed with a cold solution of 2 mg antibody in 0.5 mL PBS, pH 7.4 while stirring. The mixture was stirred at 4 °C for 30 min. Then the pH was gradually raised up to 8.6 within 4 h at r.t. The reaction mixture was left overnight in refrigerator. Next day the pH of reaction mixture was increased to 9 and the released TT was removed using a Sephadex G-25 (PD-10 column). The conjugate was fractionated on a Superose 6 (16/60) column (Amersham GE Healthcare) to separate small amount (<5%) of high molecular weight fraction (eluted on the exclusion limit of the column, Mw >500 kD), the non-bound polymer and free antibody (Fig. 2). The conjugate fraction was concentrated by ultrafiltration to 1.5 - 2.5 mL (Amicon membrane; cut off 30 kDa) and the final molecular weight profile was measured using Superose 6 (HR 10/30) column in PBS. The content of FITC (or TxR) containing polymer in concentrated conjugate fraction was measured spectrophotometrically and the content of Ab was determined by Lowry method (after subtraction of the background corresponding to polymer). Molecular weight of the conjugates was approximately 300 kDa as determined by on-line light-scattering detector (MiniDawn, Wyatt Technology Corp.).

Radioiodination of antibody and conjugates

Free antibody and copolymer antibody conjugates (P-anti-PSMA) were radioiodinated by the Iodogen method.[41,42] Briefly, 300 μl of antibody or copolymer antibody conjugates (0.5 mg/

mL in PBS, pH 7.4) were added into Iodogen pre-coated tube followed by addition of 10 μl (0.5 mCi) of $Na^{125}I$. After 5 min the labeled antibody or P-anti-PSMA were purified using a PD-10 column (Amersham GE Healthcare) pre-equilibrated with PBS containing 0.5% BSA. The specific radioactivity was 1.5μCi/μg.

Radioimmunoassay

This was performed to determine the antigen binding affinity of the free antibody and P-anti-PSMA. Briefly, cells grown in 96-wells at 80-90 % confluence were incubated with Hank's balanced salt solution containing HEPES (20 mM), NaN_3 (10 mM) and BSA (0.5%) 1 h before experiments on ice. Subsequently, cells were incubated with the above buffer containing a serial concentration of labeled and unlabeled free antibody or P-anti-PSMA on ice for 4 h. After incubation, the buffer was discarded and cells were extensively washed to remove unbound antibody or P-anti-PSMA conjugates. Cells were solubilized with 1 M NaOH for 1 h and counted for radioactivity. The values of radioactivity were analyzed using the SigmaPlot software.

Transfection

One day before transfection, 1×10^5 cells were seeded in a 35 mm Petri dish with 14 mm glass bottom microwell in the growth media. For each transfection sample, 2 μg EGFP-dynamin^{WT}, EGFP-dynamin^{K44A}, EYFP-Rab5 or EYFP-Rab7 expression plasmids, 50 pmol clathrin heavy chain siRNA or scrambled sequence (control) siRNA were diluted in 100 μl Opti-MEM I and mixed well; 5 μl Lipofectamine 2000 were diluted with 100 μl Opti-MEM I and kept for 5 min at room temperature. Then the two mixtures were combined and let to stand for 20 min at room temperature. Prior to exposure to transfection complex, cells were washed with Opti-MEM I twice and incubated with 800 μl Opti-MEM I. The 200 μl mixtures were then applied into dishes and incubated with cells for 5 h. After that, the transfection complex was discarded and cells were further incubated in growth media. Experiments were performed at 24-48 h post-transfection.

Internalization experiments

Cells were plated into sterile 35 mm Petri dish with 14 mm glass bottom microwell at a density of 1×10^5 cells per well. Cells were incubated for 2 days before internalization experiments were performed. P-anti-PSMA and Alexa Fluor 633-labeled transferrin were added to the culture medium and incubated with C4-2 cells at 37 °C for indicated time periods. Alexa Fluor 647-labeled dextran 10 kDa was added to culture medium at a concentration of 50 μg/mL and incubated with cells overnight followed by adding P-anti-PSMA. Ten minutes before microscopy, the DNA dye, Hoechst 33342, was added into dishes and incubated with cells. Then cells were washed with PBS twice and live-cell fluorescence imaging was performed immediately.

Inhibition of Internalization via endocytic pathways by selective inhibitors

Cells were incubated in serum free medium containing chlorpromazine 10 μM, wortmannin 1 μM, amiloride 10 μM, or LY294002 10 μM. Thirty minutes later, P-anti-PSMA was added into the medium (in the presence of these inhibitors) and cells incubated for another 4 h. Experiments were performed immediately after incubation.

Cholesterol depletion

To deplete cells of cholesterol, the cells were incubated in serum free medium for 1 h and then filipin 2.5 μg/mL or meviolin 10 uM was added and the cells incubated for another 30 min. Experiments were carried out at the end of incubation.

Quantitative study of uptake by flow cytometry

The cells were seeded in 12-well plates at a density of 2.5×10^5 cells per well and incubated in growth medium for 2 days (37 °C, 5% CO_2). Then the cells were incubated with conjugates at 37°C for indicated time periods. After incubation, medium containing conjugates were discarded. Cells were harvested and washed with cold PBS three times followed by flow cytometry analysis immediately. The amount of 1.0×10^4 cells was collected and analyzed for each sample.

Statistical Analysis

Statistical analysis was performed using the Student's *t* test with $*0.01 < p < 0.05$ or $**p < 0.01$ as significant difference. The experiments were performed in triplicate. Cells treated with each individual inhibitor were compared with cells without exposure to inhibitors.

Results

Synthesis and characterization of P-anti-PSMA conjugates

The synthesis of polymer precursors and of HPMA copolymer - antiPMSA antibody conjugates is shown on Fig. 1. The polymer precursor P(FITC)-(GG-TT) contained 4.9 mol% of TT, 0.4 mol% of FITC. The Mw was 42 kDa and Mw/Mn 1.5. The polymer precursor P(TxR)-(GG-TT) contained 4.8 mol% of TT, 0.35 mol% of TxR. The Mw was 50 kDa and Mw/Mn was 1.5.

The antibodies were covalently bound to HPMA copolymer precursors (P(FITC)-(GG-TT) and P(TxR)-(GG-TT)) via amide bonds formed by aminolysis of reactive thiazolidine-2-thione groups on the HPMA copolymer. This method involves the reaction of amino groups on the surface of antibody (mostly ε-amino groups of lysine). The intention was to modify the antibody only moderately to avoid conformation changes of the antibody molecule and prevent the decrease of its affinity to the target. Data from our previous study[33] showed that the amino groups in the vicinity of binding site might be less reactive than in the other part of the antibody molecule. The K_d of the conjugate prepared by aminolysis was of the same order as the original antibody[42]. The reaction conditions in this study were optimized to attach approximately three polymer chains per molecule of Ab. The weight ratio of Ab to polymer precursor was 1:1 and the concentration of Ab in the reaction mixture was 0.4 wt %. Such conditions generated only a small amount of high-molecular weight (branched or crosslinked) fraction; it was removed by SEC fractionation. The molecular weight of the conjugates calculated from the chemical composition, approximately 300 kDa, was confirmed by SEC equipped with on-line laser light scattering detector; the estimated size was 10 - 12 nm.

The characteristics of conjugates are summarized in Table 1. A typical example of the size exclusion chromatography elution profile from fractionation of conjugates using Superose 6 HR16/60 column (AKTA/FPLC, Pharmacia column, buffer PBS) is shown in Fig. 2.

Determination of the antigen binding affinity of the free antibodies and copolymer antibody conjugates

The PSMA molecule binding affinity of the antiPSMA antibodies and P-anti-PSMA conjugates were determined by radioimmunoassay in C4-2 cells highly expressing PSMA molecules. The nonspecific binding of the antibody and copolymer antibody conjugates to cells was estimated in PC-3 cells that do not express PSMA. Three monoclonal antibodies against different epitopes of PSMA and their corresponding copolymer conjugates were examined and the averages of dissociation constants (affinity) from three experiments are listed in Table 2. The binding affinities of all three antibodies were not compromised by conjugation to copolymer drug carriers. As expected, the affinity of antibodies attached to HPMA copolymer were moderately lower, but still in the same order of magnitude as the native Ab.

The HPMA copolymer anti-PSMA conjugates are endocytosed into PSMA positive cells through receptor mediated endocytosis

It has been shown previously that the mAbs 3/A12, 3/F11 and 3/E7 bind to cell adherent PSMA and are internalized.[15] To prove that P-anti-PSMA is also internalized upon the binding to PSMA, the P-anti-PSMA was incubated with C4-2 cells and PC-3 cells (Fig. 3a). P-anti-PSMA was internalized into C4-2 cells whereas uptake of P-anti-PSMA was not observed in PC-3 cells, indicating that P-anti-PSMA was internalized into C4-2 cells through PSMA-mediated endocytosis. Dextran 10 kDa, a fluid phase endocytosis marker, was co-incubated and endocytosed into PC-3 cells, demonstrating PC-3 cells' ability to execute fluid phase endocytosis, which subsequently confirmed the binding specificity of P-anti-PSMA to PMSA molecules.

The rate of uptake of P-anti-PSMA is faster than that of HPMA copolymer conjugate with non-specific IgG

As a control, an HPMA copolymer conjugate with non-specific IgG (P-IgG) was synthesized and the kinetics of P-anti-PSMA uptake was evaluated in C4-2 cells using flow cytometry (Fig. 3b). The uptake of P-anti-PSMA could be detected after 5 min of incubation of P-anti-PSMA with cells whereas the uptake of P-IgG was seen only after 1 h of incubation. The uptake of P-anti-PSMA increased more rapidly with time of incubation than that of P-IgG. It implied that uptake of P-anti-PSMA is facilitated by receptor-mediated endocytosis.

Both CME and macropinocytosis participates in the internalization of P-anti-PSMA by C4-2 cells

Mechanisms of endocytosis that might be involved in the internalization of P-anti-PSMA were investigated utilizing a variety of commonly used pathway selective inhibitors, including chlorpromazine, an inhibitor of clathrin mediated endocytosis, filipin and mevinolin, cholesterol disruption agents, inhibitors of caveolae-mediated endocytosis and amiloride, wortmannin, and LY 294004, macropinocytosis inhibitors. Endocytosis of P-anti-PSMA was diminished in cells exposed to chlorpromazine, amiloride, wortmannin and LY 294004, observed through the confocal microscopic study (Fig. 4a). The quantitative estimation of uptake of P-anti-PSMA was carried out by flow cytometry analysis (Fig. 4b). The uptake of P-anti-PSMA was inhibited by nearly 40% in cells exposed to chlorpromazine at the indicated concentration. Suppressed uptake was displayed in cells treated with three inhibitors of macropinocytosis. In particular, wortmannin, an inhibitor of phosphoinositide (PI) 3-kinases that plays a role on the regulation of macropinocytosis, reduced uptake of P-anti-PSMA nearly up to 50% at the indicated concentration. Hence, the result revealed that more than one mechanism are contributing to the internalization of P-anti-PSMA by C4-2 cells.

Down-regulation of clathrin expression diminishes the internalization of P-anti-PSMA in C4-2 cells

To further confirm that internalization of P-anti-PSMA was mediated by CME, the most well studied mechanism of receptor-mediated endocytosis, the influence of down-regulating the expression of clathrin protein, the main assembly unit of clathrin coated pits, on uptake of P-anti-PSMA was assessed. C4-2 cells were transfected with siRNA specific against clathrin heavy chain and protein expression was nearly completely abolished as detected by western blotting (data not shown). Internalization of transferrin was abolished in cells transfected with clathrin specific siRNA, as demonstrated by the disappearance of intracellular transferrin and retention of transferrin on plasma membrane. Similarly, the intracellular fluorescence of P-anti-PSMA decreased in cells transfected with clathrin specific siRNA, compared to control cells, indicating that internalization of P-anti-PSMA was regulated by clathrin (Fig. 5a). In addition, C4-2 cells were incubated with P-anti-PSMA and Alexa Fluor 633 labeled transferrin

and co-localization was analyzed. P-anti-PSMA was co-localized with transferrin (Fig. 5b). Therefore, CME is the mechanism through which P-anti-PSMA is endocytosed into C4-2 cells.

Clathrin- and caveolae-independent endocytosis also takes part in P-anti-PSMA internalization

The clathrin- and caveolae-independent pathway was also evaluated in the study. Because the clathrin- and caveolae-independent pathway is dynamin independent, a dominant negative (deficient) mutant of human dynamin (dynamin^{K44A}) has been widely used to characterize this pathway. In the present study, the wild type of dynamin (dynamin^{WT}) and dynamin^{K44A} were overexpressed as EGFP fusion protein in C4-2 cells to determine the participation of clathrin- and caveolae-independent pathway in the internalization of P-anti-PSMA. Consequently, a P-anti-PSMA conjugate labeled with TxR was synthesized and used in this study. The internalization of P-anti-PSMA was examined in overexpression-positive cells. In cells overexpressing EGFP-dynamin^{WT} (highlighted with single arrow in Fig. 5c), all the P-anti-PSMA was internalized and accumulated in the perinuclear area. However, in cells overexpressing EGFP-dynamin^{K44A} (highlighted with double arrow in Fig. 5c), retention of P-anti-PSMA at the plasma membrane coexisted with perinuclear P-anti-PSMA, indicating that endocytosis of P-anti-PSMA was not completely blocked. The intracellular P-anti-PSMA bypassed dynamin and was endocytosed. Association of P-anti-PSMA with plasma membrane indicated that the endocytosis of some of P-anti-PSMA is regulated by dynamin.

P-anti-PSMA antibody conjugates are transported to late endosomes via endosomes

Subcellular trafficking of P-anti-PSMA containing membrane vesicles was subsequently inspected. Rab small GTPases, members of the Ras superfamily, are localized at distinct membrane vesicles and are responsible for membrane vesicle formation, development and trafficking.[43-46] It is well accepted that Rab5 and Rab7 are distinct domains of early endosomes and late endosomes, respectively.[43-47] We expressed Rab5 and Rab7, fused to yellow fluorescent proteins (YFP). C4-2 cells were transfected with DNA constructs of YFP fused Rab5 and Rab7 and subsequently the trafficking of P-anti-PSMA in live cells was tracked. The P-anti-PSMA labeled with TxR was used in this study. In Fig. 6, green signals represent either Rab5 expressing early endosomes or Rab7 expressing late endosomes, while the red signal signifies membrane vesicles entrapping TxR labeled P-anti-PSMA conjugates. Membrane limited vesicles containing P-anti-PSMA were observed to co-localize with Rab5 expressing vesicles as quickly as within 15 min, demonstrating that membrane vesicles containing P-anti-PSMA rapidly mature into early endosomes. However, Rab5 gradually disappeared from vesicles containing P-anti-PSMA conjugates within 1 h. The membrane limited vesicles containing P-anti-PSMA began to mature into late endosomes after incubation for 22 min. The maturation was seen to consistently increase up to 240 min.

Discussion

Understanding the mechanism of internalization and subcellular trafficking of targeted polymer drug conjugates is of great importance for the explanation of their treatment effects and further optimization of design and synthesis. Recently, rapid advancements have been made and provided new insights into the complexity of physiological endocytic pathways. Different pathways can share a common basic pathway to which additional levels of sophistication are added.[48,49] In addition, the same cargo can be internalized through distinct endocytic mechanisms. For instance,transforming growth factor-β receptor (TGFβR) is internalized through clathrin-mediated and caveolae-mediated endocytosis.[50]

Not surprisingly, studies have shown that multiple endocytic pathways can concurrently take action when a macromolecular drug conjugate is exposed to a single type of cell. It is because

of the fact that macromolecular drug conjugates hijack the complicated physiological endocytic machinery. Rejman et al. demonstrated, using pathway inhibitors, that polyethyleneimine (PEI)/DNA polyplexes are internalized into cells through both CME and caveolae-mediated endocytosis.[51-53] It was confirmed also by using co-localization experiments.[54,55] The cellular uptake of pullulan-spermine, a cationic polysaccharide, occurred via CME and caveolae-mediated endocytosis, as proved by using appropriate inhibitors.[56] Most recently, a comprehensive model suggested that the Tat peptide simultaneously used three endocytic pathways: macropinocytosis, CME, and caveolae-mediated endocytosis.[57] In addition, a novel arginine-grafted dendritic block copolymer, R-PAMAM-PEG-PAMAM-R G5 (PPP5-R) was shown to simultaneously employ the same three pathways.[58]

This study revealed that P-anti-PSMA is internalized by C4-2 cells through multiple endocytic pathways. CME is a major pathway of C4-2 cells internalizing P-anti-PSMA. Clathrin coated pits are formed by the assembly of cytosolic coat proteins, the main assembly unit being clathrin. Clathrin is a three-legged structure formed by three heavy chains, each with a tightly associated clathrin light chain. We disrupted the formation of clathrin-coated pits by siRNA-mediated down regulation of clathrin heavy chain protein expression. This genetic approach together with co-localization of P-anti-PSMA with transferrin and internalization in the presence of chlorpromazine inhibitor strongly indicated that CME is one of the mechanisms by which P-anti-PSMA molecules are internalized. This conclusion is indirectly supported by the biochemical characteristics of PSMA. Transferrin is the best-characterized ligand of CME. The entire sequence of PSMA is related to the transferrin receptor (TfR) with 20% homology. The overall structure and domain organization of TfR and PSMA are similar, as revealed by the crystal structure of PSMA.[59] It was proposed that small cytoplasmic motifs of TfR1 and PSMA, YXRF and MXXXL, respectively, solely regulate their uptake by endocytosis.[60]

In addition to CME, a fraction of P-anti-PSMA was internalized into C4-2 cells through macropinocytosis. Distinct from CME, macropinocytosis is initiated by plasma membrane protrusion to the external milieu, a process of extensive plasma membrane reorganization. Macropinocytosis occurs spontaneously or upon the stimulation of growth-factor-receptor.[32,61,62] Presumably, a large volume of extracellular fluid or a macromolecule of large size triggers macropinocytosis. However, no regulation has been found to control the size or morphology of the enclosed macropinosome. Recently, involvement of actin filaments in macropinocytosis and regulation of macropinocytosis by PI3-kinases have been studied extensively.[32,35] Inhibition of PI3K abolishes macropinocytosis of macromolecules (mostly in closing of cup invagination) and fusion of macropinosomes. It also interrupts the membrane protrusion in some cells. The physico-chemical characteristics of cargo that is endocytosed by macropinocytosis remain unknown. However, as a common mechanism of fluid phase endocytosis, macropinocytosis has recently been discovered to actively participate in the internalization of a variety of macromolecules, such as intact protein, cell penetrating peptides, synthetic polymers and nanoparticles.[62-66] Using three specific inhibitors of macropinocytosis, we verified that macropinocytosis takes part in internalization of P-anti-PSMA.

Clathrin- and caveolae-independent endocytosis was another mechanism found participating in the internalization of P-anti-PSMA. This endocytic pathway is least well defined. Due to the independency of clathrin and caveolin, this pathway was defined by the absence of dynamin recruitment. In fact, the evidence of the existence of this pathway originated from the analysis of cells expressing a temperature-sensitive dynamin mutant. Dynamin is a multidomain GTPase that assembles into a `collar' around the neck of vesicle invagination to mediate the release of vesicles into the cytoplasm. It is involved in the scission of a wide range of vesicles such as clathrin-coated vesicles and caveolae.[36]

Most recently, there was a report that dextran 10 kDa also adopts clathrin- and caveolae-independent pathway to be endocytosed into cells.[22] We thus inspected the similarity between dextran and P-anti-PSMA internalization. In EGFP-Dynamin^{K44A} positive cells, the internalization of dextran 10 kDa did not remarkably decline, similarly to P-anti-PSMA (data not shown). This supports the conclusion that a portion of P-anti-PSMA internalization is dynamin-independent, similarly to dextran 10 kDa, and occurs via the clathrin- and caveolae-independent pathway.

The clathrin coated pit formation and regulation, as well as trafficking of membrane vesicles derived from CME, are relatively well understood. Clathrin coated pits enclosing cargoes pinching off from plasma membranes are subsequently transported to early endosomes. Sorting occurs at this stage. Some lipid and protein cargoes that possess housekeeping features are recycled back to the plasma membrane through recycling endosomes or the trans-Golgi network. Other molecules, destined to be degraded, congregate rapidly within multivesicular endosomes, which move along the microtubule network to late endosomes. Late endosomes act as another level sorting station from which most of the molecules presumably are transported to lysosomes for degradation.[48, 49]

The route of macropinosomes transport in the endocytic pathway remains unclear. There is a tendency to agree that macropinosomes rapidly develop into early endosomes.[67-69] Nevertheless, there is a discrepancy whether macropinosomes or derived early endosomes continue to progress into late endosomes and lysosomes.[67-69] Similarly, the membrane vesicles enclosing cargoes from clathrin-,caveolae-independent entry might fuse with endosomes after pitching off. However, the final destination of cargo remains unsolved.

Trafficking of P-anti-PSMA is anticipated to be sophisticated based on the complexity of its entry into C4-2 cells. Hence, we decided to dissect and pick up the mainframe of P-anti-PSMA trafficking that is of importance for the design and optimization of macromolecular drug conjugates. We visualized the early endosomes and late endosomes by overexpression of Rab GTPase proteins. It was able to provide more conclusive results compared to commonly used lysotracker due to the high specificity. We found that some of membrane vesicles trapping P-anti-PSMA rapidly developed or fused to endosomes after budding off. Some of membrane vesicle trapping P-anti-PSMA rapidly fused to late endosomes and it seemed that they consistently remained in Rab7 positive membrane vesicles for prolonged time (24 h). Presumably, these Rab7 positive membrane vesicles ultimately mature into lysosomes. Interestingly, we found that in a specific period of time P-anti-PSMA disappeared from early endosomes, while it accumulated in late endosomes. It is well in agreement with the report from Zerial and coworkers that Rab5 is converted to Rab7 during early-to-late endosome trafficking.[38] Based on these results, polymer-drug conjugates can be designed containing drugs attached via either endosome escaping spacers or lysosome enzymes cleavable spacers for the best of treatment effects.

Overall, our results demonstrated that multiple mechanisms could be involved in the endocytosis of antibody-polymer conjugates. Trafficking of membrane vesicles trapping targeted macromolecular drug conjugates can be traced, which will guide the design and optimization of targeted macromolecular drug conjugates.

Acknowledgment

We thank Dr. Diane McVey Ward (University of Utah) and Dr. Xiaowei Zhuang (Howard Hughes Medical Institute, Harvard University) for their generous gifts of EGFP-dynamin^{WT}, EGFP-dynamin^{K44A}, EYFP-Rab5 and EYFP-Rab7. The research was supported in part by NIH grant RO1 CA132831 from the National Cancer Institute (to J.K.).

Abbreviation

PSMA, prostate specific membrane antigen; HPMA, *N*-(2- hydroxypropyl)methacrylamide; P-anti-PSMA, HPMA (*N*-(2-hydroxypropyl)methacrylamide) copolymer - anti-PSMA antibody conjugates; P-IgG, HPMA copolymer conjugate with non-specific IgG: CME: clathrin-mediated endocytosis; Dynamin K44A, dominant-negative mutant of dynamin.

References

(1). Shiah JG, Dvořák M, Kopečková P, Sun Y, Peterson CM, Kopeček J. Biodistribution and antitumour efficacy of long-circulating *N*-(2-hydroxypropyl)methacrylamide copolymer-doxorubicin conjugates in nude mice. Eur. J. Cancer 2001;37:131–139. [PubMed: 11165140]

(2). Allen TM. Ligand-targeted therapeutics in anticancer therapy. Nat. Rev. Cancer 2002;2:750–763. [PubMed: 12360278]

(3). Reichert JM, Rosensweig CJ, Faden LB, Dewitz MC. Monoclonal antibody successes in the clinic. Nat. Biotechnol 2005;23:1073–1078. [PubMed: 16151394]

(4). Shiah JG, Sun Y, Kopečková P, Peterson CM, Straight RC, Kopeček J. Combination chemotherapy and photodynamic therapy of targetable *N*-(2-hydroxypropyl)methacrylamide copolymer-doxorubicin/mesochlorin e_6-OV-TL 16 antibody immunoconjugates. J. Controlled Release 2001;74:249–253.

(5). Lu ZR, Kopečková P, Kopeček J. Polymerizable Fab' antibody fragments for targeting of anticancer drugs. Nat. Biotechnol 1999;17:1101–1104. [PubMed: 10545917]

(6). Peer D, Karp JM, Hong S, Farokhzad OC, Margalit R, Langer R. Nanocarriers as an emerging platform for cancer therapy. Nat. Nanotechnol 2007;2:751–760. [PubMed: 18654426]

(7). Seymour LW, Ferry DR, Anderson D, Hesslewood S, Julyan PJ, Poyner R, Doran J, Young AM, Burtles S, Kerr DJ. Hepatic drug targeting: Phase I evaluation of polymer-bound doxorubicin. J. Clin. Oncol 2002;20:1668–1676. [PubMed: 11896118]

(8). Lu ZR, Shiah JG, Kopečková P, Kopeček J. Polymerizable Fab' antibody fragment targeted photodynamic cancer therapy in nude mice. STP Pharma Sci 2003;13:69–75.

(9). Fair WR, Israeli RS, Heston WD. Prostate-specific membrane antigen. Prostate 1997;32:140–148. [PubMed: 9215402]

(10). Silver DA, Pellicer I, Fair WR, Heston WD, Cordon-Cardo C. Prostate-specific membrane antigen expression in normal and malignant human tissues. Clin. Cancer Res 1997;3:81–85. [PubMed: 9815541]

(11). Israeli RS, Powell CT, Corr JG, Fair WR, Heston WD. Expression of the prostate-specific membrane antigen. Cancer Res 1994;54:1807–1811. [PubMed: 7511053]

(12). Kawakami M, Nakayama J. Enhanced expression of prostate-specific membrane antigen gene in prostate cancer as revealed by in situ hybridization. Cancer Res 1997;57:2321–2324. [PubMed: 9192800]

(13). Wright GL Jr. Grob BM, Haley C, Grossman K, Newhall K, Petrylak D, Troyer J, Konchuba A, Schellhammer PF, Moriarty R. Upregulation of prostate-specific membrane antigen after androgen-deprivation therapy. Urology 1996;48:326–334. [PubMed: 8753752]

(14). Liu H, Moy P, Kim S, Xia Y, Rajasekaran A, Navarro V, Knudsen B, Bander NH. Monoclonal antibodies to the extracellular domain of prostate-specific membrane antigen also react with tumor vascular endothelium. Cancer Res 1997;57:3629–3634. [PubMed: 9288760]

(15). Elsässer-Beile U, Wolf P, Gierschner D, Bühler P, Schultze-Seemann W, Wetterauer U. A new generation of monoclonal and recombinant antibodies against cell-adherent prostate specific membrane antigen for diagnostic and therapeutic targeting of prostate cancer. Prostate 2006;66:1359–1370. [PubMed: 16894535]

(16). Wolf P, Gierschner D, Bühler P, Wetterauer U, Elsässer-Beile U. A recombinant PSMA-specific single-chain immunotoxin has potent and selective toxicity against prostate cancer cells. Cancer Immunol. Immunother 2006;55:1367–1373. [PubMed: 16547705]

(17). Wolf P, Alt K, Bühler P, Katzenwadel A, Wetterauer U, Tacke M, Elsässer-Beile U. Anti-PSMA immunotoxin as novel treatment for prostate cancer? High and specific antitumor activity on human prostate xenograft tumors in SCID mice. Prostate 2008;68:129–138. [PubMed: 18044731]

(18). Bühler P, Wolf P, Gierschner D, Schaber I, Katzenwadel A, Schultze-Seemann W, Wetterauer U, Tacke M, Swamy M, Scxhamel WW, Elsässer-Beile U. A bispecific diabody directed against prostate-specific membrane antigen and CD3 induces T-cell mediated lysis of prostate cancer cells. Cancer Immunol. Immunother 2008;57:43–52. [PubMed: 17579857]

(19). Lupold SE, Hicke BJ, Lin Y, Coffey DS. Identification and characterization of nuclease-stabilized RNA molecules that bind human prostate cancer cells via the prostate-specific membrane antigen. Cancer Res 2002;62:4029–4033. [PubMed: 12124337]

(20). McNamara JO, Andrechek ER, Wang Y, Viles KD, Rempel RE, Gilboa E, Sullenger BA, Giangrande PH. Cell type-specific delivery of siRNAs with aptamer-siRNA chimeras. Nat Biotechnol 2006;24:1005–1015. [PubMed: 16823371]

(21). Farokhzad OC, Cheng J, Teply BA, Sherifi I, Jon S, Kantoff PW, Richie JP, Langer R. Targeted nanoparticle-aptamer bioconjugates for cancer chemotherapy in vivo. Proc Natl Acad Sci U S A 2006;103:6315–6320. [PubMed: 16606824]

(22). Cheng J, Teply BA, Sherifi I, Sung J, Luther G, Gu FX, Levy-Nissenbaum E, Radovic-Moreno AF, Langer R, Farokhzad OC. Formulation of functionalized PLGA-PEG nanoparticles for in vivo targeted drug delivery. Biomaterials 2007;28:869–876. [PubMed: 17055572]

(23). Dhar S, Gu FX, Langer R, Farokhzad OC, Lippard SJ. Targeted delivery of cisplatin to prostate cancer cells by aptamer functionalized Pt(IV) prodrug-PLGA-PEG nanoparticles. Proc Natl Acad Sci U S A 2008;105:17356–17361. [PubMed: 18978032]

(24). Wullner U, Neef I, Eller A, Kleines M, Tur MK, Barth S. Cell-specific induction of apoptosis by rationally designed bivalent aptamer-siRNA transcripts silencing eukaryotic elongation factor 2. Curr Cancer Drug Targets 2008;8:554–565. [PubMed: 18991566]

(25). Chu TC, Marks JW 3rd, Lavery LA, Faulkner S, Rosenblum MG, Ellington AD, Levy M. Aptamer:toxin conjugates that specifically target prostate tumor cells. Cancer Res 2006;66:5989–5992. [PubMed: 16778167]

(26). Farokhzad OC, Khademhosseini A, Jon S, Hermmann A, Cheng J, Chin C, Kiselyuk A, Teply B, Eng G, Langer R. Microfluidic system for studying the interaction of nanoparticles and microparticles with cells. Anal Chem 2005;77:5453–5459. [PubMed: 16131052]

(27). Bagalkot V, Zhang L, Levy-Nissenbaum E, Jon S, Kantoff PW, Langer R, Farokhzad OC. Quantum dot-aptamer conjugates for synchronous cancer imaging, therapy, and sensing of drug delivery based on bi-fluorescence resonance energy transfer. Nano Lett 2007;7:3065–3070. [PubMed: 17854227]

(28). Conner SD, Schmid SL. Regulated portals of entry into the cell. Nature 2003;422:37–44. [PubMed: 12621426]

(29). Lakadamyali M, Rust MJ, Zhuang X. Ligands for clathrin-mediated endocytosis are differentially sorted into distinct populations of early endosomes. Cell 2006;124:997–1009. [PubMed: 16530046]

(30). Pelkmans L. Secrets of caveolae- and lipid raft-mediated endocytosis revealed by mammalian viruses. Biochim. Biophys. Acta 2005;1746:295–304. [PubMed: 16126288]

(31). Kirkham M, Parton RG. Clathrin-independent endocytosis: new insights into caveolae and noncaveolar lipid raft carriers. Biochim. Biophys. Acta 2005;1746:349–363. [PubMed: 16440447]

(32). Swanson JA. Shaping cups into phagosomes and macropinosomes. Nat. Rev. Mol. Cell Biol 2008;9:639–649. [PubMed: 18612320]

(33). Haucke V. Cargo takes control of endocytosis. Cell 2006;127:35–37. [PubMed: 17018271]

(34). Perret E, Lakkaraju A, Deborde S, Schreiner R, Rodriguez-Boulan E. Evolving endosomes: how many varieties and why? Curr. Opin. Cell Biol 2005;17:423–434. [PubMed: 15975780]

(35). Lindmo K, Stenmark H. Regulation of membrane traffic by phosphoinositide 3-kinases. J. Cell Sci 2006;119:605–614. [PubMed: 16467569]

(36). Praefcke GJ, McMahon HT. The dynamin superfamily: universal membrane tubulation and fission molecules? Nat. Rev. Mol. Cell Biol 2004;5:133–147. [PubMed: 15040446]

(37). Bareford LM, Swaan PW. Endocytic mechanisms for targeted drug delivery. Adv. Drug Delivery Rev 2007;59:748–758.

(38). Richardson SC, Wallom KL, Ferguson EL, Deacon SP, Davies MW, Powell AJ, Piper RC, Duncan R. The use of fluorescence microscopy to define polymer localisation to the late endocytic compartments in cells that are targets for drug delivery. J. Controlled Release 2008;127:1–11.

(39). Šubr V, Ulbrich K. Synthesis and properties of new *N*-(2-hydroxypropyl)methacrylamide copolymers containing thiazolidine-2-thione. React. Funct. Polym 2006;66:1525–1538.

(40). Omelyanenko V, Kopečková P, Gentry C, Kopeček J. Targetable HPMA copolymeradriamycin conjugates. Recognition, internalization, and subcellular fate. J. Controlled Release 1998;53:25–37.

(41). Fraker PJ, Speck JC Jr. Protein and cell membrane iodinations with a sparingly soluble chloroamide, 1,3,4,6-tetrachloro-3a,6a-diphrenylglycoluril. Biochem. Biophys. Res. Commun 1978;80:849–857. [PubMed: 637870]

(42). Omelyanenko V, Kopečková P, Gentry C, Shiah JG, Kopeček J. HPMA copolymeranticancer drug-OV-TL16 antibody conjugates. 1. Influence of the method of synthesis on the binding affinity to OVCAR-3 ovarian carcinoma cells in vitro. J. Drug Targeting 1996;3:357–373.

(43). Pfeffer S. A model for Rab GTPase localization. Biochem. Soc. Trans 2005;33:627–630. [PubMed: 16042559]

(44). Zerial M, McBride H. Rab proteins as membrane organizers. Nat. Rev. Cell Biol 2001;2:107–117.

(45). Pfeffer S, Aivazian D. Targeting Rab GTPases to distinct membrane compartments. Nat. Rev. Mol. Cell Biol 2004;5:886–896. [PubMed: 15520808]

(46). Pfeffer S. Filling the Rab GAP. Nat. Cell Biol 2005;7:856–857. [PubMed: 16136184]

(47). Rink J, Ghigo E, Kalaidzidis Y, Zerial M. Rab conversion as a mechanism of progression from early to late endosomes. Cell 2005;122:735–749. [PubMed: 16143105]

(48). Bonifacino JS, Rojas R. Retrograde transport from endosomes to the trans-Golgi network. Nat. Rev. Mol. Cell Biol 2006;7:568–579. [PubMed: 16936697]

(49). van der Goot FG, Gruenberg J. Intra-endosomal membrane traffic. Trends Cell Biol 2006;16:514–521. [PubMed: 16949287]

(50). Le Roy C, Wrana JL. Clathrin- and non-clathrin-mediated endocytic regulation of cell signalling. Nat. Rev. Mol. Cell Biol 2005;6:112–126. [PubMed: 15687999]

(51). Rejman J, Bragonzi A, Conese M. Role of clathrin- and caveolae-mediated endocytosis in gene transfer mediated by lipo- and polyplexes. Mol. Ther 2005;12:468–474. [PubMed: 15963763]

(52). Rejman J, Conese M, Hoekstra D. Gene transfer by means of lipo- and polyplexes: role of clathrin and caveolae-mediated endocytosis. J. Liposome Res 2006;16:237–247. [PubMed: 16952878]

(53). Hoekstra D, Rejman J, Wasungu L, Shi F, Zuhorn I. Gene delivery by cationic lipids: in and out of an endosome. Biochem. Soc. Trans 2007;35:68–71. [PubMed: 17233603]

(54). von Gersdorff K, Sanders NN, Vandenbroucke R, De Smedt SC, Wagner E, Ogris M. The internalization route resulting in successful gene expression depends on both cell line and polyethylenimine polyplex type. Mol. Ther 2006;14:745–753. [PubMed: 16979385]

(55). van der Aa MA, Huth US, Häfele SY, Schubert R, Oosting RS, Mastrobattista E, Hennink WE, Peschka-Süss R, Koning GA, Crommelin DJ. Cellular Uptake of Cationic Polymer-DNA Complexes Via Caveolae Plays a Pivotal Role in Gene Transfection in COS-7 Cells. Pharmaceutical Res 2007;24:1590–1598.

(56). Kanatani I, Ikai T, Okazaki A, Jo J, Yamamoto M, Imamura M, Kanematsu A, Yamamoto S, Ito N, Ogawa O, Tabata Y. Efficient gene transfer by pullulan-spermine occurs through both clathrin- and raft/caveolae-dependent mechanisms. J. Controlled Release 2006;116:75–82.

(57). Duchardt F, Fotin-Mleczek M, Schwarz H, Fischer R, Brock R. A comprehensive model for the cellular uptake of cationic cell-penetrating peptides. Traffic 2007;8:848–866. [PubMed: 17587406]

(58). Kim TI, Baek JU, Yoon JK, Choi JS, Kim K, Park JS. Synthesis and characterization of a novel arginine-grafted dendritic block copolymer for gene delivery and study of its cellular uptake pathway leading to transfection. Bioconjugate Chem 2007;18:309–317.

(59). Davis MI, Bennett MJ, Thomas LM, Bjorkman PJ. Crystal structure of prostate-specific membrane antigen, a tumor marker and peptidase. Proc. Natl. Acad. Sci. U. S. A 2005;102:5981–5986. [PubMed: 15837926]

(60). Rajasekaran SA, Anilkumar G, Oshima E, Bowie JU, Liu H, Heston W, Bander NH, Rajasekaran AK. A novel cytoplasmic tail MXXXL motif mediates the internalization of prostate-specific membrane antigen. Mol. Biol. Cell 2003;14:4835–4845. [PubMed: 14528023]

(61). Amyere M, Mettlen M, Van Der Smissen P, Platek A, Payrastre B, Veithen A, Courtoy PJ. Origin, originality, functions, subversions and molecular signalling of macropinocytosis. Int. J. Med. Microbiol 2002;291:487–494. [PubMed: 11890548]

(62). Jones AT. Macropinocytosis: searching for an endocytic identity and role in the uptake of cell penetrating peptides. J. Cell Mol. Med 2007;11:670–684. [PubMed: 17760832]

(63). Mennesson E, Erbacher P, Piller V, Kieda C, Midoux P, Pichon C. Transfection efficiency and uptake process of polyplexes in human lung endothelial cells: a comparative study in non-polarized and polarized cells. J Gene Med 2005;7:729–738. [PubMed: 15759254]

(64). Gratton SE, Napier ME, Ropp PA, Tian S, DeSimone JM. Microfabricated particles for engineered drug therapies: elucidation into the mechanisms of cellular internalization of PRINT particles. Pharm Res 2008;25:2845–2852. [PubMed: 18592353]

(65). Kaplan IM, Wadia JS, Dowdy SF. Cationic TAT peptide transduction domain enters cells by macropinocytosis. J Control Release 2005;102:247–253. [PubMed: 15653149]

(66). Magzoub M, Sandgren S, Lundberg P, Oglecka K, Lilja J, Wittrup A, Goran Eriksson LE, Langel U, Belting M, Graslund A. N-terminal peptides from unprocessed prion proteins enter cells by macropinocytosis. Biochem Biophys Res Commun 2006;348:379–385. [PubMed: 16893522]

(67). Kerr MC, Lindsay MR, Luetterforst R, Hamilton N, Simpson F, Parton RG, Gleeson PA, Teasdale RD. Visualisation of macropinosome maturation by the recruitment of sorting nexins. J. Cell Sci 2006;119:3967–3980. [PubMed: 16968745]

(68). Schnatwinkel C, Christoforidis S, Lindsay MR, Uttenweiler-Joseph S, Wilm M, Parton RG, Zerial M. The Rab5 effector Rabankyrin-5 regulates and coordinates different endocytic mechanisms. PLoS Biol 2004;2:E261. [PubMed: 15328530]

(69). Hamasaki M, Araki N, Hatae T. Association of early endosomal autoantigen 1 with macropinocytosis in EGF-stimulated A431 cells. Anat. Rec. A Discov Mol. Cell Evol. Biol 2004;277:298–306. [PubMed: 15052657]

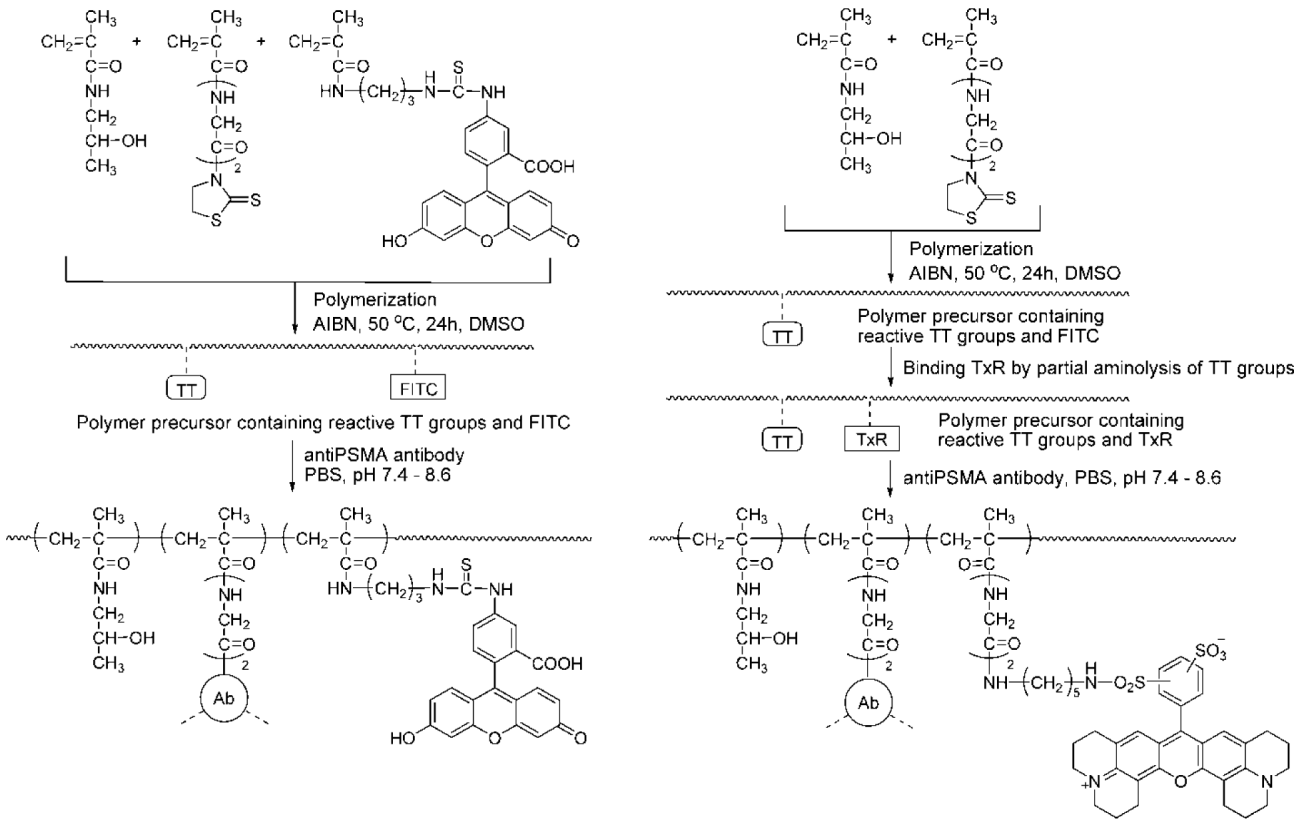

Figure 1.
Scheme of synthesis of HPMA copolymer - anti-PMSA antibody conjugates (P-anti-PMSA).

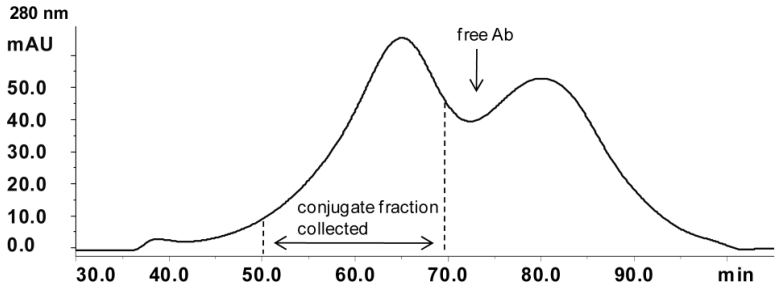

Figure 2.
Typical example of the SEC elution profile of P-anti-PMSA using Superose 6 HR16/60 column (AKTA/FPLC, buffer PBS).

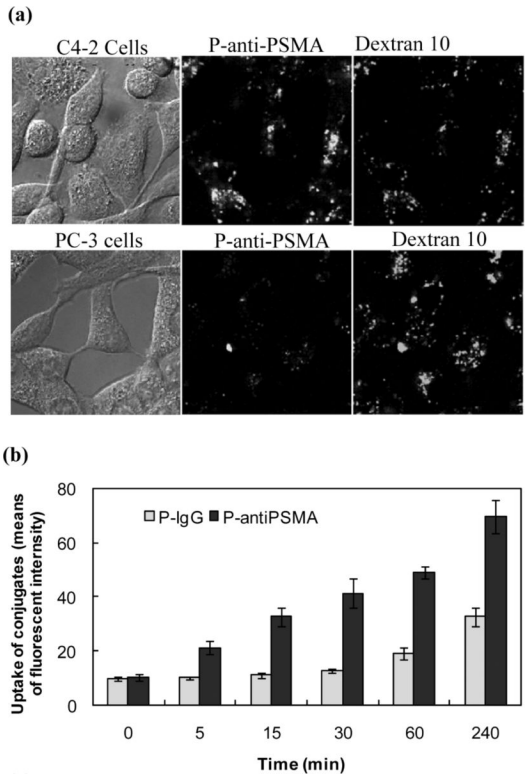

Figure 3.

(a) Internalization of P-anti-PSMA in PSMA positive C4-2 and PSMA negative PC-3 cells. Cells were pre-incubated with Alexa 647 labeled dextran 10 kDa, a fluid phase pinocytosis marker, for 16 h at 37 °C and then exposed to P-anti-PSMA for 2 h*[1]. Medium containing the conjugate was washed out followed by confocal microscopy study*[2]. The pictures were from one confocal Z slice*[3]. *1: The concentration of P-anti-PSMA used in the whole study was 12 $\times 10^{-3}$ mg/mL of antiPSMA and 6.4×10^{-3} mg/mL of copolymer; *2: Images were taken in live cells in the whole study; *3: All pictures shown were from one confocal Z slice taken using an Olympus confocal microscope (FV 1000). (b) Kinetic study of uptake of P-anti-PSMA by C4-2 cells. The cells were incubated with either P-anti-PSMA or HPMA copolymer - non-specific IgG conjugate (P-IgG) using comparable amounts of antiPSMA and IgG, as well as FITC, for indicated period of time, followed by flow cytometry analysis.

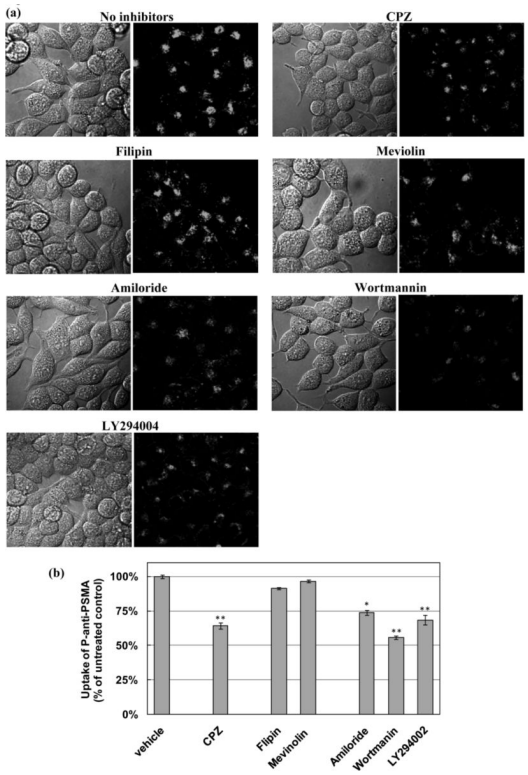

Figure 4.

Inhibition of P-anti-PSMA uptake using pathway selective inhibitors. Cells were pretreated with chlorpromazine (10 μM), an inhibitor of clathrin - mediated endocytosis; filipin (2.5 μg/mL) and mevinolin (10 μM), inhibitors of caveolae-mediated endocytosis; amiloride (10 μM), wortmannin (10 μM), and LY 294004 (10 μM), macro-pinocytosis inhibitors, for 0.5 h. The cells were incubated for another 2 h with P-anti-PSMA in the presence of inhibitors. (a) Confocal micro-scopy images of cells demonstrate diminished endocytosis. (b) Quantitative analysis of uptake by flow cytometry was carried out after incubation. The percentages of uptake of each sample in comparison to control are shown. The experiments were performed in triplicate and asterisks (*) and (**) indicate statistically significant differences ($0.01 < p < 0.05$) and ($p < 0.01$) compared to control, respectively.

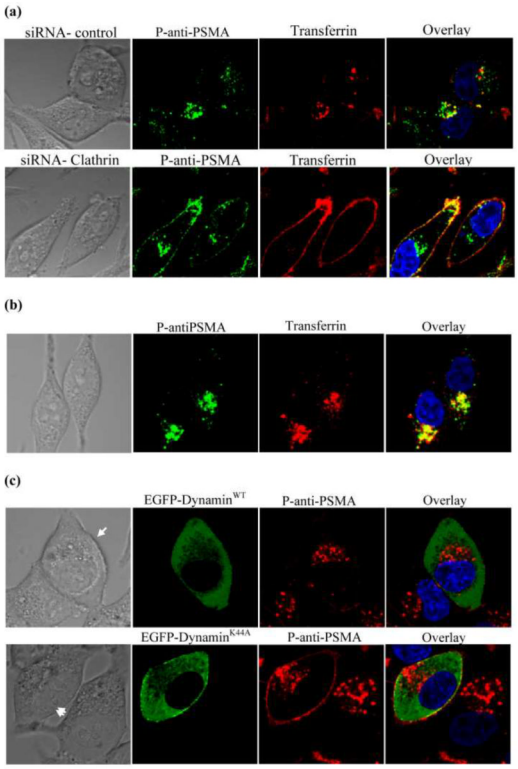

Figure 5.

(a) Inhibition of the endocytosis of transferrin and P-anti-PSMA using clathrin-specific siRNA. C4-2 cells were transfected with clathrin heavy chain siRNA and incubated for 48 h, followed by incubation with transferrin and P-anti-PSMA for 1 h. (b) Co-localization of P-anti-PSMA with transferrin. P-anti-PSMA and Alexa fluor 633 labeled transferrin were co-incubated for 1 h. (c) Endocytosis of P-anti-PSMA was not completely abolished by dynamin deficiency. Cells were transfected with EGFP-Dynamin^{WT}, or EGFP-Dynamin^{K44A} - a dynamin-deficient mutant that has been shown to block both clathrin- and caveolae-mediated endocytosis. After transfection, cells were incubated for 2 days and then exposed to P-anti-PSMA and transferrin.

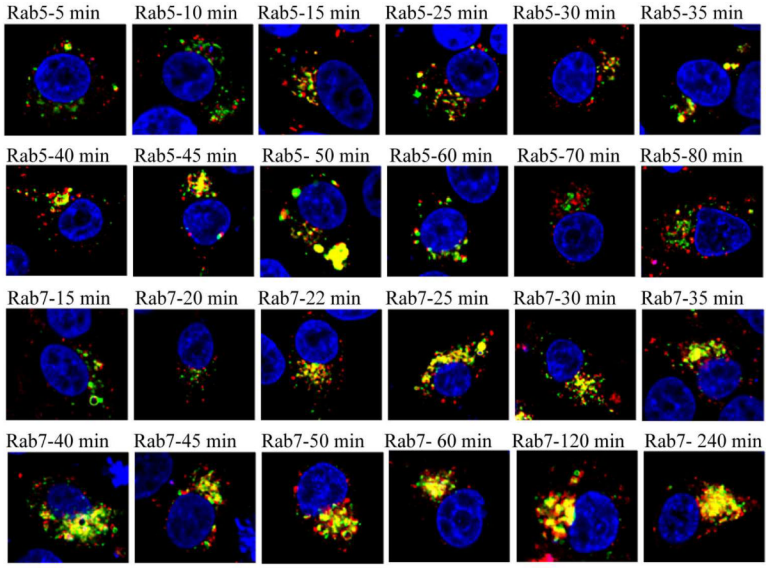

Figure 6.

Subcellular trafficking of P-anti-PSMA conjugates. C4-2 cells were transfected with DNA constructs of YFP fused Rab5 and Rab7 by using lipofectamine 2000 according to manufacturer's recommendation. After 24 h, cells were incubated with P-anti-PSMA for indicated period of time. Membrane vesicles containing P-anti-PSMA were observed quickly to fuse to endosomes but rapidly disappeared from early endosomes. P-anti-PSMA containing vesicles begun to fuse to late endosomes after incubation for 22 min. The fusion was seen to consistently increase up to 240 min.

Table 1

Characterization of P-anti-PSMA

Conjugate	Polymer precursor	Antibody	Conjugate composition[b] (wt%)	
			Ab	polymer
P(FITC)-3F11	P(FITC)-(GG-TT)	3F11	63.9	36.1
P(FITC)-3E7	P(FITC)-(GG-TT)	3E7	61.8	38.2
P(TxR)-3A12	P(TxR)-(GG-TT)	3A12	62.0	38.0
P(FITC)-IgG[a]	P(FITC)-(GG-TT)	IgG	66.5	33.5

[a] Human IgG

[b] Molecular ratio of Ab : polymer was calculated for all conjugates as ~ 1 : 3

Table 2

The dissociation affinities of free anti-PSMA antibodies and P-anti-PSMA

Sample	3A/12	3F/11	3E/7	P-anti-PSMA(3A/12)	P-anti-PSMA(3F/11)	P-anti-PSMA(3E/7)
Kd (nM)	7.5	6.8	12	24	16	42

The dissociation affinities of three different isoforms of anti-PSMA antibodies and their corresponding copolymer conjugates in C4-2 cells were measured and the averages of dissociation affinities from three experiments were listed. The error of determination was approximately ± 25%.